

BAYESIAN INVESTIGATION OF ISOCHRONE CONSISTENCY USING THE OLD OPEN CLUSTER NGC 188¹

Shane Hills

*Department of Physics, Engineering Physics and Astronomy, Queen's University, Kingston, ON
K7L 3N6 Canada*

`shane.hills@queensu.ca`

Ted von Hippel

*Department of Physical Sciences, Embry-Riddle Aeronautical University, Daytona Beach, FL
32114, USA*

`ted.vonhippel@erau.edu`

Stéphane Courteau

*Department of Physics, Engineering Physics and Astronomy, Queen's University, Kingston, ON
K7L 3N6 Canada*

`courteau@astro.queensu.ca`

and

Aaron M. Geller

*Center for Interdisciplinary Exploration and Research in Astrophysics (CIERA) and Department
of Physics and Astronomy, Northwestern University, 2145 Sheridan Rd, Evanston, IL 60208, USA*

*Department of Astronomy and Astrophysics, University of Chicago, 5640 S. Ellis Avenue,
Chicago, IL 60637, USA*

`a-geller@northwestern.edu`

ABSTRACT

This paper provides a detailed comparison of the differences in parameters derived for a star cluster from its color-magnitude diagrams depending on the filters and models used. We examine the consistency and reliability of fitting three widely-used stellar evolution models to fifteen combinations of optical and near-IR photometry for the old open cluster NGC 188. The optical filter response curves match those of the theoretical systems and are thus not the source of fit inconsistencies. NGC 188 is ideally suited to the present study thanks to a wide variety of high-quality photometry and

available proper motions and radial velocities which enable us to remove non-cluster members and many binaries. Our Bayesian fitting technique yields inferred values of age, metallicity, distance modulus, and absorption as a function of the photometric band combinations and stellar models. We show that the historically-favored three band combinations of *UBV* and *VRI* can be meaningfully inconsistent with each other and with longer baseline datasets such as *UBVRIJHK_S*. Differences among model sets can also be substantial. For instance, fitting Yi et al. (2001) and Dotter et al. (2008) models to *UBVRIJHK_S* photometry for NGC 188 yields the following cluster parameters: age = $\{5.78 \pm 0.03, 6.45 \pm 0.04\}$ Gyr, $[\text{Fe}/\text{H}] = \{+0.125 \pm 0.003, -0.077 \pm 0.003\}$ dex, $(m - M)_V = \{11.441 \pm 0.007, 11.525 \pm 0.005\}$ mag, and $A_V = \{0.162 \pm 0.003, 0.236 \pm 0.003\}$ mag, respectively. Within the formal fitting errors, these two fits are substantially and statistically different. Such differences amongst fits using different filters and models are a cautionary tale regarding our current ability to fit star cluster color-magnitude diagrams. Additional modeling of this kind, with more models and star clusters, and future GAIA parallaxes are critical for isolating and quantifying the most relevant uncertainties in stellar evolutionary models.

Subject headings: Methods: statistical – open clusters and associations: individual (NGC 188)

1. Introduction

Stellar evolution is a mature field with numerous successes, perhaps the most important of which is the ability to determine star cluster ages. These ages are the basis for our understanding of the star formation histories of the Milky Way and other galaxies and provide a cornerstone of modern astrophysics. Yet, the ages that we derive for star clusters suffer from well-known observational and theoretical uncertainties (e.g. Kurucz 2002; Asplund et al. 2009; Pereira et al. 2013), as well as difficulties in matching observations to theory (e.g. Flower 1996; von Hippel et al. 2002; Dotter et al. 2008). We focus on these data-model comparisons, which have historically been exacerbated by subjective fitting techniques and an unknown sensitivity on filter choice. Generally, researchers adjust a handful of model parameters, testing for their impact in color-magnitude diagrams (CMDs), until a good match is found. This approach is subjective as different research groups matching the same multi-band data set to the same models might not derive matching cluster parameters. Furthermore, studies of the same cluster by different groups may differ in their choice of photometric bands. Yet, the sensitivity of cluster parameters to different filter combinations remains poorly constrained, though past studies (e.g. Figure 10 of Sarajedini et al.

¹This is paper 64 of the WIYN Open Cluster Study (WOCS).

1999; Grocholski & Sarajedini 2003) indicate that stellar modeling results do depend on the choice of photometric bands.

In this paper, we refine the data-model interface by employing an objective Bayesian fitting technique and using it to study the sensitivity of fits between stellar models and common subsets of $UBVRIJHK_S$ photometry. We focus our investigation on the old open cluster NGC 188 because of the available, extensive, high-quality photometry and the high-quality proper-motion and radial-velocity data, which enable us to remove most non-cluster members and binaries from the CMD. By focusing on one cluster, we can perform an extensive CMD analysis with many filter combinations and three stellar evolution codes, yet our results are necessarily limited to clusters with parameters similar to NGC 188. Needless to say, this approach ought to motivate similar studies with a broad suite of stellar evolution models and wide range of stellar clusters.

We first describe the photometry, radial velocities, and proper motions for NGC 188 in section §2. We then present the Bayesian statistical technique used for our analysis in section §3, and apply it to different photometry band combinations in section §4. Our results and conclusions, with a view to future investigations and an extension of this analysis to other clusters, are presented in sections §5 and §6, respectively.

2. Observations

For the observational data of NGC 188, we rely on the homogenized $UBVRI$ photometry of Stetson, McClure, & Vandenberg (2004), which were derived from nearly a dozen independent observational studies, combined with cluster membership probabilities from four proper-motion studies. The sheer number of previous photometric and astrometric studies of NGC 188 over the last fifty years (Sandage 1962; Sharov 1965; Cannon 1968; Eggen & Sandage 1969; Uggren et al. 1972; McClure & Twarog 1977; Caputo et al. 1990; Dinescu et al. 1996; von Hippel & Sarajedini 1998; Sarajedini et al. 1999; Platais et al. 2003) demonstrate the considerable interest in this cluster largely because it is well-populated, relatively unreddened, and one of the oldest known open clusters. We supplement the optical photometry with 2MASS JHK_S photometry from Skrutskie et al. (2006).

Along with the photometry, we take advantage of the multi-epoch radial-velocity data from Geller et al. (2008; 2009; and additional observations from the continuation of their radial-velocity survey). This radial-velocity sample contains at least three observations for nearly every solar-type star from ~ 1.5 mag below the cluster turn-off up to the tip of the giant branch (~ 0.95 to $1.15 M_\odot$) within a 1° diameter region centered on NGC 188 (corresponding to a radius of ~ 17 pc or roughly 13 core radii), and spans a monitoring baseline of more than a decade for many stars. The radial-velocity data enable us to further remove non-cluster members and many of the cluster binary stars in what is otherwise a busy, field-star-contaminated CMD. The radial-velocity survey’s ability to detect binaries depends primarily on the orbital periods because of the

monitoring baseline of the survey, and is also sensitive to the binary mass ratios, eccentricities, and orbital inclination (see Geller et al. 2012). Monte Carlo completeness analysis indicates that 63% of the solar-type binaries with orbital periods $< 10^4$ days (of all mass ratios, eccentricities, and inclinations) are detected in this survey, whereas very few with longer periods are detected. Geller et al. (2012) estimate the hard-binary versus soft-binary boundary for NGC 188 to be about 10^6 days, so presumably some fraction of long-period solar-type binaries remain undetected. Yet, removing this large sample of binaries is particularly useful for accurate cluster quantities because such binaries can confuse the location of the main sequence turn-off and substantially broaden the main sequence. Our analysis technique (see below) includes fitting binaries of all mass ratios (regardless of orbital periods, eccentricities, etc.), yet our results are more accurate when we can remove these binaries in advance.

We obtain a well-populated CMD with 248 stars, each with full $UBVRIJHK_S$ photometry and a variety of cluster membership metrics, by combining the optical photometry and proper-motion data from Stetson et al. (2004) with the infrared photometry from Skrutskie et al. (2006), as well as the radial-velocity measurements from Geller et al. (2012), including all star-by-star uncertainties in every parameter. Figure 1 shows the CMD for NGC 188.

We considered multiple ways to incorporate both the proper-motion and radial-velocity cluster membership probabilities for this study, though none are ideal. Simply multiplying these independent probabilities yields very low membership probabilities (i.e. $\sim 20\%$ or less) for some stars, potentially due to uncertainties in one set of data or the other. This reduces the importance of those stars to the fit. The alternative of taking the greatest cluster membership value would neglect potentially important information contained in whichever method was ignored. We explored a few other techniques of combining cluster memberships. Fortunately, our tests with various datasets showed that the results were insensitive to the specific techniques used to combine membership probabilities. As a result we employ a simple arithmetic mean of the proper-motion and radial-velocity probabilities for our cluster membership probabilities.

3. Statistical Method

For the purposes of this study, we require an objective and precise technique to fit stellar isochrones to cluster photometry. The software suite BASE-9² (**B**ayesian **A**nalysis of **S**tellar **E**volution with **9** Parameters) fits our requirements well. (For a full discussion of the method, software, and the capabilities of BASE-9, see von Hippel et al. 2006; DeGennaro et al. 2009; van Dyk et al. 2009; and Stein et al. 2013.) BASE-9 compares stellar evolution models (listed below) to photometry in any combination of photometric bands for which there are data and models. Of particular benefit for our study, BASE-9 accounts for individual errors for every data point,

²BASE-9 is freely available from the second author.

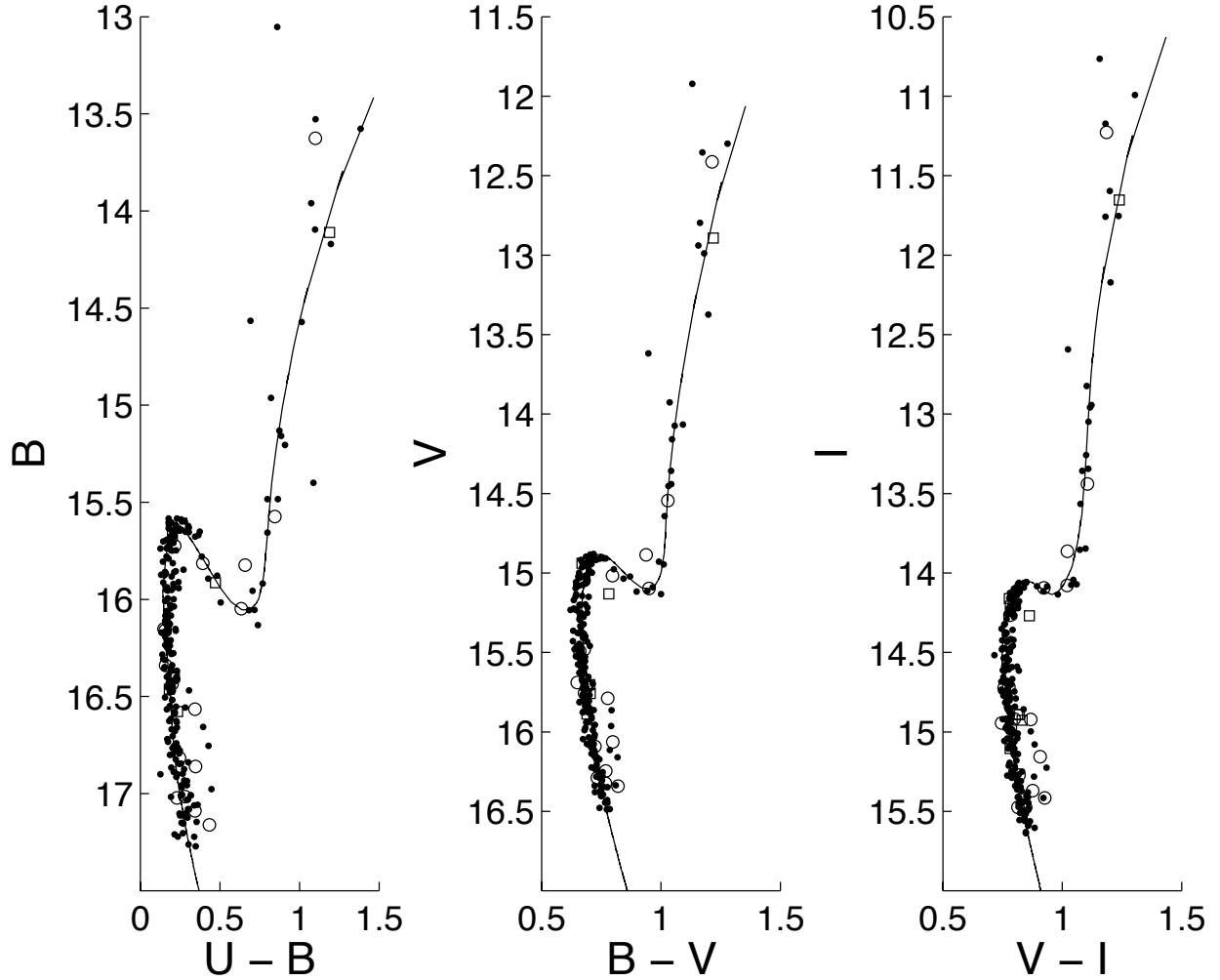


Fig. 1.— CMDs for NGC 188 in a range of optical bands. The point types correspond to the assigned cluster membership probability for each star (filled circles have membership probabilities greater than 0.9, open circles indicate between 0.7 and 0.9 probability, open squares show probabilities less than 0.7). These probabilities result from the arithmetic mean of membership probabilities from Stetson et al. (2004) (based on proper motions) and Geller et al. (2008) (based on radial velocities). The data are overplotted with the mean fitted isochrone (solid line) found by BASE-9 in its $UBVRI$ photometry fit to Yi et al. (2001) models (see section 4).

incorporates cluster membership probabilities from proper motions or radial velocities, and cluster metallicity from spectroscopic studies. As per above, we incorporated membership probabilities from both proper motions and radial velocities using an arithmetic mean.

BASE-9 uses a computational technique known as Markov chain Monte Carlo (MCMC) to derive the Bayesian joint posterior probability distribution for up to six parameter categories (cluster

age, metallicity, helium content, distance, and reddening, and optionally for white dwarf studies, a parameterized initial-final mass relation) and brute-force numerical integration for three parameter categories (stellar mass on the zero-age main sequence, binarity, and cluster membership). The last three of these parameter categories include one parameter per star whereas the first six parameter categories refer to the entire cluster. This study includes no white dwarfs and we therefore do not use the initial-final mass relation. Additionally, among the isochrone sets we employ, there is a fixed relationship between metallicity and helium content. We are also not concerned with the individual stellar masses in this study. BASE-9 marginalizes over the parameters that are not of direct interest to us, yielding the four cluster-wide parameters (age, metallicity, distance, absorption) pertinent to this work.

BASE-9 allows us to take advantage of prior information, where available, to constrain parameters. For this problem, the results are insensitive to the exact choice of reasonable priors. We chose priors with a Gaussian shape in the logarithmic quantities with mean values from the photometric study of Sarajedini et al. (1999), specifically $[\text{Fe}/\text{H}] = -0.03$, $(m - M)_V = 11.44$, and $A_V = 0.3$. Yet, we set the uncertainties on these priors to be broad enough that they would not unreasonably constrain our fits, given our current knowledge of these values, specifically $\sigma([\text{Fe}/\text{H}]) = 0.3$, $\sigma((m - M)_V) = 0.3$, and $\sigma(A_V) = 0.1$. We performed sensitivity tests on these priors and found that reasonable values for these prior standard deviations yielded negligible differences compared to the variation caused by different filter combinations.

We have adopted the stellar evolution models of Girardi et al. (2000), Yi et al. (2001), and Dotter et al. (2008). The Girardi et al. isochrones span the age range of 63 Myr to nearly 18 Gyr from metal-free stars up to $[\text{Fe}/\text{H}] = +0.2$. The Yi et al. isochrones span 1 Myr to 20 Gyr from $[\text{Fe}/\text{H}] = -3.7$ to nearly $+0.8$. The Dotter et al. isochrones span 250 Myrs to 15 Gyrs over a metallicity range of $[\text{Fe}/\text{H}] = -2.5$ to $+0.5$. All of these parameter ranges easily bracket NGC 188, which has near solar abundance and is approximately 6 Gyrs old.

4. Results

4.1. Posterior Probability Distributions and Best-Fit Isochrones

It is common practice to run MCMC routines such as BASE-9 (von Hippel et al. 2006) long enough to collect 10,000 uncorrelated samples. In many cases, if the MCMC steps are too small, the excursions through parameter space are correlated, yielding fewer independent samples. In such a case, we then keep only every n -th iteration, where n is set such that subsequent stored iterations are uncorrelated. While there is no well-defined number of appropriate samples, 10,000 is usually more than sufficient to determine the shape of every posterior distribution function, including those with extended tails or multi-modality. At the other extreme, the Central Limit Theorem dictates that approximately 30 uncorrelated samples are sufficient for a normal distribution (e.g. Hogg & Tanis 2005). Before running a particular dataset against a specific set of models, we do

not know if the posterior distributions will be Gaussian shaped or more complex, so we take the conservative approach and initially assume complex posterior distributions and run BASE-9 for 10,000 uncorrelated iterations.

Each of the uncorrelated samples from BASE-9 is an allowable fit of a particular family of stellar evolution models to the cluster data, given the photometric errors, probabilities of membership, etc. In order to obtain the posterior probability distributions for the four cluster parameters of interest (age, $[\text{Fe}/\text{H}]$, $(m - M)_V$, A_V), we marginalize the sampling history derived by BASE-9 by binning along the parameter axis of interest. Many of these distributions are nearly Gaussian in shape, however some are substantially non-Gaussian. The root cause of the non-Gaussian distributions is that stellar evolution is intrinsically non-linear, so that, for example, Gaussian errors in photometry do not propagate as Gaussian errors in cluster age. One of the strengths of the Bayesian technique is that it recovers the posterior parameter distributions, which provide an informative indication of uncertainty that often cannot be captured with a simple (frequentist) best-fit parameter with error bars. Figure 2 presents posterior probability distributions for two different filter combinations.

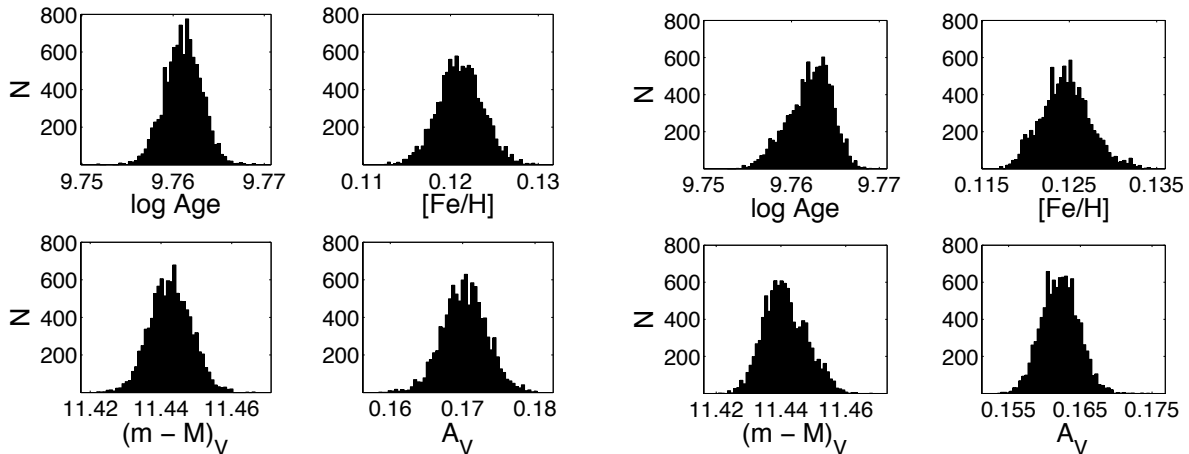


Fig. 2.— **(Left)** Posterior probability distributions for log age, $[\text{Fe}/\text{H}]$, $(m - M)_V$, and A_V using $UBVR$ photometry and Yi et al. (2001) isochrones. **(Right)** Posterior probability distributions for these same cluster parameters based on $UBVR I J H K_S$ photometry and Yi et al. (2001) isochrones. The log age distribution is noticeably skewed, which is also the case with the Dotter et al. (2008) models.

As an example of the fits derived by BASE-9, we overplot in Figure 1 an isochrone derived from the mean parameters for the Yi et al. (2001) stellar evolution models fit to the $UBVR$ dataset, the posterior distributions of which are plotted in the four panels on the left in Figure 2. These particular distributions are symmetric, so the mean and median cluster parameters are essentially identical. In some cases they are different, yet typically with the precision of this technique and the quality of this dataset there are no differences to the human eye between isochrones based on the mean versus the median fit. The Bayesian approach also reminds us that there is no single best

fit isochrone, but rather a range of probabilistically acceptable isochrones. It is the distribution of these acceptable isochrones that forms the posterior distributions. Any overplotted isochrone is at best just a representative example drawn from that distribution. In fact, isochrones created from summary statistics such as mean or median parameters may not be truly representative if the distributions are substantially non-Gaussian because that simultaneous combination of parameters may fit the data with low probability.

4.2. Differences Among Commonly Used Filters

Before embarking on a detailed comparison of model fits as a function of subsets of the adopted *UBVRIJHK_S* filters, we take a brief look into the subject of filter prescriptions. Because observatories have different versions of these filters and stellar isochrones do not include all possible such filters, we sought to check the sensitivity of BASE-9 fits to a few filter prescriptions. Specifically, we test three variations on the *B* filter from Bessell (1990) and Maiz-Apellaniz (2006) by using BASE-9 to fit simulated *UB*, *UBV*, and *UBVRI* photometry based on these filter prescriptions. These sensitivity tests are clearly not exhaustive. Rather, they are meant to provide an estimate of the sensitivity isochrone fits have to filter prescriptions.

We employed Girardi et al. models, available at <http://stev.oapd.inaf.it/cgi-bin/cmd> (see Bressan et al. 2012), to generate isochrones with $Z = 0.0144$, $Y = 0.27387$, $[M/H] = -0.01$, and age = 6.41 Gyr, along with either of the two *B* filters of Bessell (1990) or the *B* filter of Maiz-Apellaniz (2006). These model parameters are almost identical to one set of our NGC 188 fits (see next section). To these isochrones, we added a distance modulus of 11.38 and offset the absorption for all bands according to Table 3 of Cardelli, Clayton, & Mathis (1989) for $A_V = 0.17$. We then created approximately the same number of simulated stars along this sequence as we have stars in our NGC 188 database and added appropriately-sized photometric errors.

We recovered the four cluster parameters for these simulated clusters with BASE-9. Table 1 presents a comparison among these fits, with offsets between any particular fit and the fit to the first Bessell prescription for that filter combination. Uncertainties derived from combining in quadrature the one standard deviation ranges for both posterior probability distributions are listed in parentheses. The differences between the two Bessell fits in the *UB* case are zero within the errors. They are statistically significant in the *UBVRI* case, but small. For the *UBV* case, the differences are substantial and amount to 1.03 ± 0.12 Gyr, though the other cluster parameters are more stable. The differences between the fit to the first Bessell *B*-filter prescription and that of Maiz-Apellaniz is substantial and statistically significant in all three cases, particularly for ages. These differences arise from assuming that the *B* filter used in the simulated observations is the same as the *B* filter used in the fit, highlighting the importance of incorporating the correct filter prescriptions whenever possible, and particularly when deriving absolute cluster parameters.

While filter prescriptions fundamentally matter, we defer related studies to a future paper

given that the comparisons among filters presented in the next section are *differential*. We have a high-quality data set that undoubtedly suffers small systematics (estimated by Stetson, McClure, & Vandenberg (2004) to be ≤ 0.02 mag for the optical data). We will use subsets of filters from this same data set repeatedly and compare these data to the same models, looking for differences among fits as a function of filter within a given stellar model set.

4.3. Cluster Parameters as a Function of Selected Filters

We fit three widely used stellar evolution models (Girardi et al. 2000; Yi et al. 2001; Dotter et al. 2008) to fifteen combinations of optical/near-IR photometry. These three isochrone sets consistently rely on Johnson-Cousins *UBVRI* as defined by Bessell (1979, 1990). We acknowledge a filter mismatch with the Yi et al. and Girardi et al. models for which a K_S filter response is not available. Because the *JHK* age constraints are not as reliable as those at optical wavelengths, due partly to the lack of isochrone morphology information in these red bandpasses, we do not report *JHK* fits nor attempt a K_S to K transformation, which would introduce additional uncertainty.

Our BASE-9 fits produced too many fits to present all the posterior distributions. Additionally, we require summary statistics in order to compare among these models and filters. Therefore, we adopt box-and-whisker plots to provide both summary statistics and capture the degree of non-Gaussianity in the distributions. In box-and-whisker plots, the central line delineates the median of the distribution and the box edges indicate the 25th and 75th percentiles. The whiskers extend out to the most extreme non-outliers, and outliers are plotted individually. A data point is considered an outlier if it is smaller than $q_1 - \frac{3}{2}(q_3 - q_1)$ or greater than $q_3 + \frac{3}{2}(q_3 - q_1)$, where q_1 and q_3 are the 25th and 75th percentiles, respectively.

In Figures 3 through 6, we plot the derived cluster parameters for NGC 188 for each of the three stellar evolution models and each of the fifteen filter combinations of our study. Focusing first on Figure 3, we see that the Dotter et al. models converge to ages that are internally consistent within the full range of the age posterior distributions, except for *VRI*. Fewer of these fits are consistent within $\pm 1 \sigma$, with *VRI*, *UB*, and *VI* being the clearest examples. Though the entire posterior distribution for *VI* is wide, its systematic offset from most of the other filter combinations is troubling given the common use of this filter pair. The age fits based on the Yi et al. results show two age families that are again broadly consistent within the full posterior ranges, though not within $\pm 1 \sigma$ in many cases. The age fits based on the Girardi et al. models are displayed only for completeness. These models do not incorporate Equivalent Evolutionary Points (EEPs, Bertelli et al. 1994), and so BASE-9 has difficulty interpolating these models, particularly on the sub-giant branch and base of the red giant branch. This causes artificially narrow age locking in about half of all cases. These model fits are still useful, however, as they show that even with a fixed (and reasonable) age, different filter combinations may yield different values for the other cluster parameters (see below), which further tests the reliability of fits as a function of the filter combination that one employs. Because of the EEP issue with the Girardi et al. models, we do not

report the fitted values based on these models in the conclusions or abstract.

Which ages are most reliable? Because stellar structure models are better at predicting bolometric luminosity than T_{eff} , which is not a physical quantity in any case, and because stellar atmosphere models are imperfect, we expect stellar evolution models to more poorly predict flux in a particular passband than the sum of all available passbands. The full range of optical and near-IR filters from U through K_S does not complete the stellar spectrum, of course, but for G and K stars, which dominate NGC 188’s CMD, the vast majority of the flux is within these filters. We therefore take the $UBVRIJHK_S$ fits as our reference standard and expect that they will yield more accurate results than any other combination of filters with less wavelength coverage. We derive significantly different ages from fitting Dotter et al. models (mean = 6.45, median = 6.45, $q_1 = 6.43$, $q_3 = 6.48$, $\sigma=0.04$, all in Gyr) and Yi et al. models (mean = 5.78, median = 5.79, $q_1 = 5.76$, $q_3 = 5.81$, $\sigma=0.03$, all in Gyr). Figure 3 also shows that while the distributions for some fits can be extremely narrow, with the central 50% of the distribution spanning less than 0.1 Gyr for a cluster ~ 6 Gyr old, or a precision better than 2%, different age fits within a model set can span nearly 1 Gyr in some cases, though typically differ by ~ 0.4 Gyr.

Figure 4 shows that the fitted metallicity distributions display patterns similar to those of Figure 3, though the offsets in metallicity are now so small that most are below the resolution limit of current spectroscopic analyses. In this case, the differences are astrophysically unimportant, yet demonstrate that more filters tend to yield tighter metallicity constraints and that some filter combinations can provide statistically distinct fits at least for some models. For example, the $BVIK$, BVI , and VRI Dotter et al. solutions differ significantly from the other precise fits, as do two of these three combinations with the other two stellar evolution models. It is also evident that the BVI fit is not just the linear multiplication of the BV and VI fits.

Figure 5 presents distance moduli fits for these model and filter combinations. In the full eight-filter cases, the fitted precisions are excellent, with 50% of the posterior distribution spanning ≤ 0.009 mag. Yet, clearly, distances cannot be derived this precisely when the distance moduli vary by 0.1 to 0.2 mag among different filter and isochrone fits.

Finally, Figure 6 presents absorption (A_V) fits. For NGC 188, A_V is typically modest at ~ 0.2 mag. The UBV and UB fits tend to be the least consistent with all the other filter combinations, which is to be expected because the U band is the most sensitive to interstellar absorption. On the other hand, it is surprising that the UBV and UB fits are mutually inconsistent for all three isochrone sets and that while UB fits yield high absorption, UBV appears to yield overly low absorption. Instead, these results more likely indicate that models in U and B yield poorer fits to the data, likely due to the narrow wavelength baseline and the difficulty of obtaining good stellar atmospheres in the near-ultraviolet.

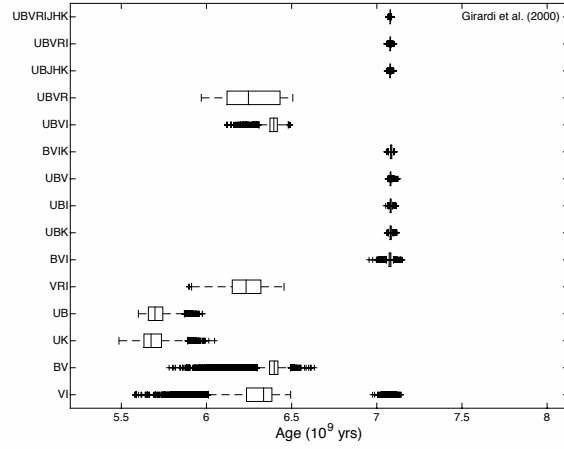
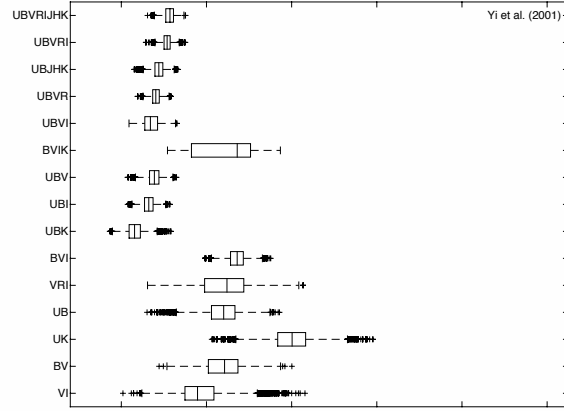
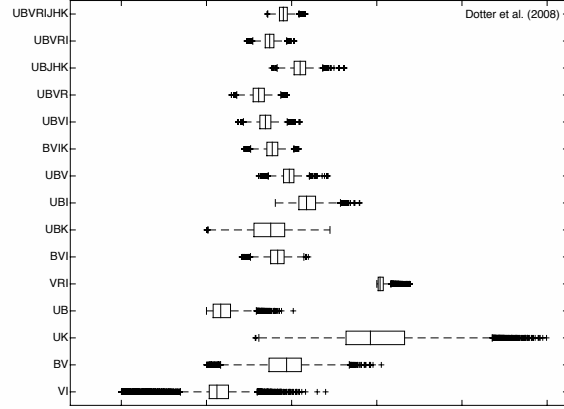


Fig. 3.— Box-and-whisker plots for age across fifteen photometric band combinations. Top: Dotter et al. (2008) isochrone models; Middle: Yi et al. (2001) isochrone models; Bottom: Girardi et al. (2000) isochrone models.

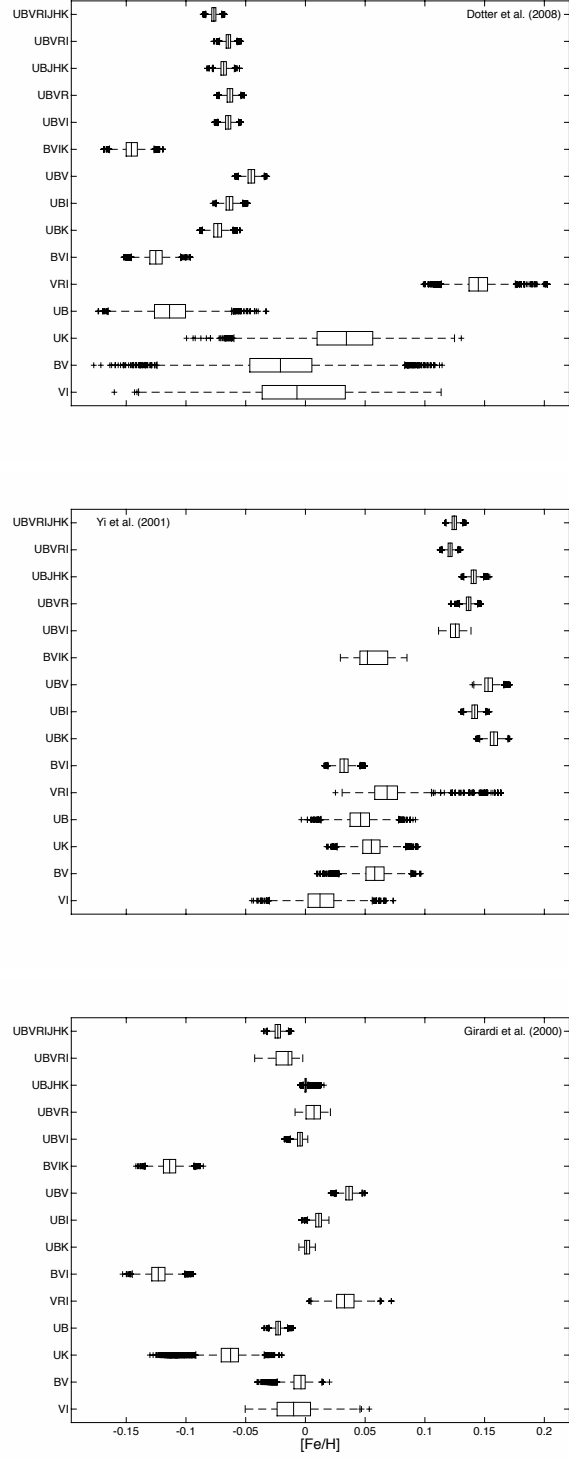


Fig. 4.— Similar to Figure 3, but for $[\text{Fe}/\text{H}]$.

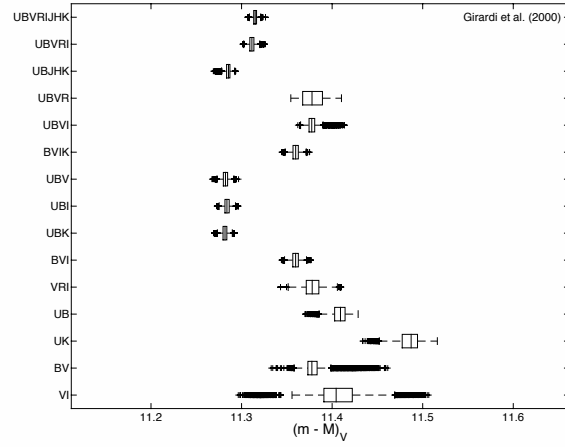
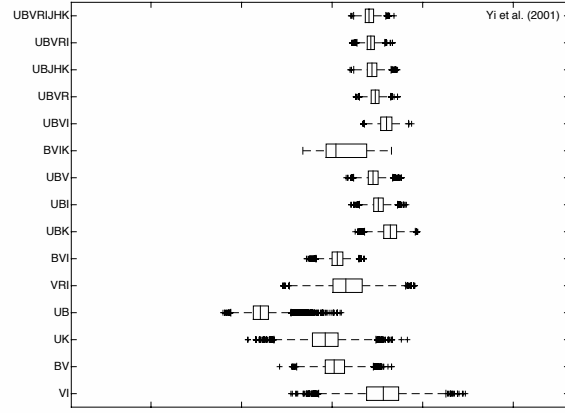
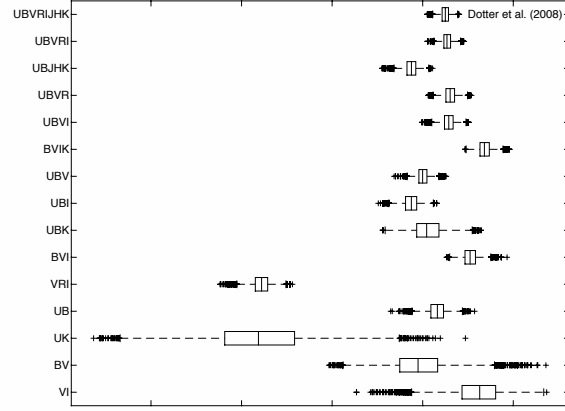


Fig. 5.— Similar to Figure 3, but for $(m - M)_V$.

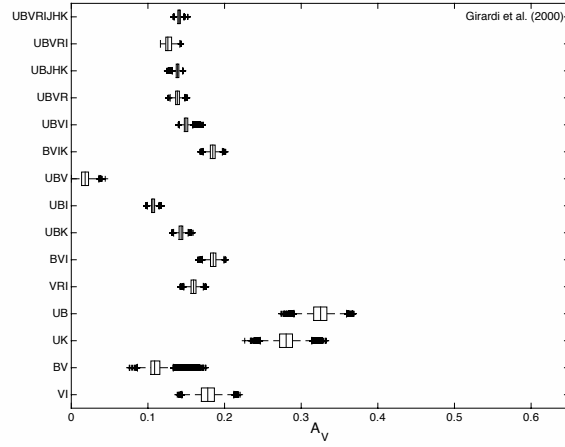
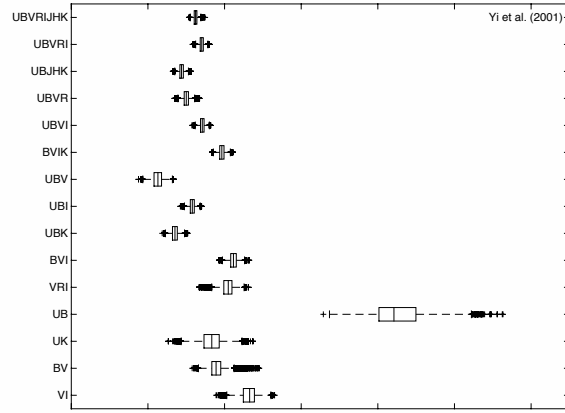
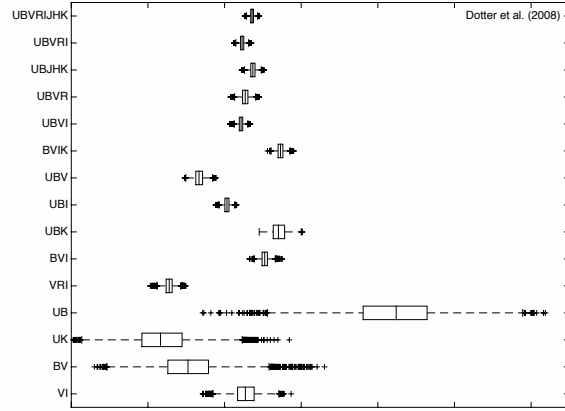


Fig. 6.— Similar to Figure 3, but for A_V .

5. Discussion

NGC 188 is one of the best-studied clusters on the sky. It has modest reddening, a well-constrained metallicity, and reliable cluster membership probabilities. In addition, this data set contains little photometric contamination from binaries making it a good test case for the sensitivity of isochrone fits to various filter combinations. Figures 3 through 6 demonstrate that different filter combinations can yield meaningfully different ages and distances. Specifically, we find that the two wide-baseline filter combinations $UBVRIJHK_S$ and $UBVRI$ generally yield consistent results. The infrared filters are thus less essential. There is somewhat weaker consistency between $UBVRIJHK_S$ and $UBVRI$ on the one hand and $UBJHK_S$, $UBVR$, and $UBVI$ on the other hand, or among these latter three combinations. The other filter combinations yield less consistent results, though these deviations may often be lost in the widths of their substantially larger posterior distributions. Of particular historical note are the filter combinations UBV , used extensively for photo-electric photometry, and VRI , used extensively for CCD photometry. In this study, we find that UBV fits are consistent with the eight-filter fits in age, somewhat less consistent in metallicity and distance, and most inconsistent in absorption. The VRI fits are substantially less consistent with the eight-filter fits than the UBV fits for all four of these cluster parameters. At this point we can only affirm that these results apply to NGC 188 and probably other solar metallicity clusters with similar ages. We do not expect these same disparity patterns for younger clusters whose bluer stars drive the age fits and where bluer filters play a driving force in isochrone fitting. Additionally, the consistency of fits may be improved for globular clusters because low metallicity atmospheres are easier to model.

The inconsistencies inherent to isochrone fitting also highlight that stellar models still suffer from incomplete treatment of important physics. Because any stellar evolution model has a specific relationship between turn-off mass and age, and because mass is precisely connected to luminosity, the other three cluster parameters can act as free parameters, at least within some constrained bounds. To match the luminosity of the turn-off, BASE-9 can adjust the distance with appropriate additional adjustments in absorption and metallicity. The freedom of adjusting multiple cluster parameters may bury the evidence that would be most helpful in determining which stellar models and which wavelength ranges are most problematic. In principle, highly constrained isochrone fits for a wide range of clusters with different ages and metallicities may reveal the magnitude of the underlying physical problems, whether they be assumptions about convection at the base of the giant branch or line blanketing in stellar atmospheres or perhaps other physics that we may be less concerned about.

In any case, the European Space Agency’s GAIA satellite mission heralds a new era where at least one large source of uncertainty, cluster distances, can be highly constrained with great precision and accuracy. Locking down cluster distances with reliable parallaxes to $24 \mu\text{as}$ (expected for a $V \leq 15$ star with G star colors, see <http://sci.esa.int/gaia/47354-fact-sheet>), could constrain the distance to NGC 188 (at ~ 2 kpc) considerably. There are 27 stars in our CMD with $V \leq 15$ and 83 stars with $V \leq 15.5$. The expected parallax accuracy of 4.8% per star at 2 kpc improves by

at least a factor of $\sqrt{27-1} \approx 5$, and could be more than 10 times higher once all observed stars are properly included, meaning that the distance to NGC 188 will be known to at least 0.5-1%. This corresponds to an uncertainty of 0.01-0.02 mag in distance modulus, which is more than an order of magnitude improvement over the range of the fits in Figure 5.

6. Conclusions

Using the Bayesian statistical stellar evolution package BASE-9, we fit the well-studied old open cluster NGC 188 for age, $[\text{Fe}/\text{H}]$, $(m - M)_V$, and A_V under fifteen different photometry regimes, using a range of filters and wavelength baselines. We argue that employing all eight filters, and thus the widest baseline, yields the most precise and accurate fits. The five-filter *UBVRI* combination was nearly as good. However, other filter combinations often gave inconsistent results with each other and with the eight-filter results. These inconsistencies can span 1 Gyr, though 0.4 Gyr differences, or $\sim 6\%$, are more typical for NGC 188.

Differences amongst the model sets can also be substantial. Specifically, fitting Yi et al. (2001) and Dotter et al. (2008) models to the eight-filter data, yields the following mean cluster parameters: age = $\{5.78 \pm 0.03, 6.45 \pm 0.04\}$ Gyr, $[\text{Fe}/\text{H}] = \{+0.125 \pm 0.003, -0.077 \pm 0.003\}$ dex, $(m - M)_V = \{11.441 \pm 0.007, 11.525 \pm 0.005\}$ mag, and $A_V = \{0.162 \pm 0.003, 0.236 \pm 0.003\}$ mag, respectively. With such small formal fitting errors, these two fits are substantially and statistically different. The differences amongst fitted parameters using different filters and models is a cautionary tale regarding our current ability to fit star cluster CMDs.

Our case study of NGC 188 should be extended to other stellar clusters to cover the widest range of cluster parameters. In doing so, the match between the filter response functions for the theoretical evolutionary models and the actual observations must be confirmed to eliminate a common source of systematic error.

We thank Elliot Robinson for his help with BASE-9 development. This material is based upon work supported by the National Aeronautics and Space Administration under Grant NNX11AF34G issued through the Office of Space Science. SC acknowledges support through a Discovery grant from the Natural Sciences and Engineering Research Council of Canada. AMG is funded by a National Science Foundation Astronomy and Astrophysics Postdoctoral Fellowship under Award No. AST-1302765.

REFERENCES

- Asplund, M., Grevesse, N., Sauval, A. J., & Scott, P. 2009, *ARA&A*, 47, 481
- Bertelli, G., Bressan, A., Chiosi, C., Fagotto, F., & Nasi, E. 1994, *A&AS*, 106, 275

- Bessell, M. S. 1979, *PASP*, 91, 589
- Bessell, M. S. 1990, *PASP*, 102, 1181
- Bressan, A., Marigo, P., Girardi, L., et al. 2012, *MNRAS*, 427, 127
- Cannon, R. D. 1968, Ph.D. thesis, Cambridge Univ.
- Caputo, F., Chieffi, A., Castellani, V., Collados, M., Martinez Roger, C., & Paez, E. 1990, *AJ*, 99, 261
- Cardelli, J. A., Clayton, G. C., & Mathis, J. S. 1989, *ApJ*, 345, 245
- DeGennaro, S., von Hippel, T., Jefferys, W. H., Stein, N., van Dyk, D. A., & Jeffery, E. 2009, *ApJ*, 696, 12
- Dinescu, D. I., Girard, T. M., van Altena, W. F., Yang, T.G., & Lee, Y.W. 1996, *AJ*, 111, 1205
- Dotter, A., Chaboyer, B., Jevremovic, D., Kostov, V., Baron, E., & Ferguson, J. W. 2008, *ApJS*, 178, 89
- Eggen, O., & Sandage, A. 1969, *ApJ*, 158, 669
- Flower, P. J. 1996, *ApJ*, 469, 355
- Geller, A. M. & Mathieu R. D. 2012, *AJ*, 144, 54
- Geller, A. M., Mathieu, R. D., Harris, H. C., & McClure, R. D. 2008, *AJ*, 135, 2264
- Geller, A. M., Mathieu, R. D., Harris, H. C., & McClure, R. D. 2009, *AJ*, 137, 3743
- Girardi, L., Bressan, A., Bertelli, G., & Chiosi, C. 2000, *A&AS*, 141, 371
- Grocholski, A. J., & Sarajedini, A. 2003, *MNRAS*, 345, 1015
- Hogg, R. V., & Tanis, E. A. 2005, *Probability and Statistical Inference*, 7th Edition (Prentice Hall)
- Kurucz, R. L. 2002, *BaltA*, 11, 101
- Maiz-Apellaniz, J. 2006, *AJ*, 131, 1184
- McClure, R. D., & Twarog, B. A. 1977, *ApJ*, 214, 111
- Pereira, T. M. D., Asplund, M., Collet, R., Thaler, I., Trampedach, R., & Leenaarts, J. 2013, *A&A*, 554, 118P
- Platais, I., KozhurinaPlatais, V., Mathieu, R., Girard, T. M., & van Altena, W. F. 2003, *AJ*, 126, 2922
- Sandage, A. 1962, *ApJ*, 135, 333
- Sarajedini, A., von Hippel, T., KozhurinaPlatais, V., & Demarque, P. 1999, *AJ*, 118, 2894
- Sharov, A. S. 1965, *Soob. Shternberg*, 142, 20
- Skrutskie, M. F., et al. 2006, *AJ*, 131, 1163
- Stein, N., van Dyk, D. A., von Hippel, T., DeGennaro, S., Jeffery, E. J., & Jefferys, W. H. 2013, *Statistical Analysis and Data Mining*, 6, 34

- Stetson, P. B., McClure, R. D., & VandenBerg, D. A. 2004, *PASP*, 116, 1012
- Upgren, A. R., Mesrobian, W. S., & Kerridge, S. J. 1972, *AJ*, 77, 74
- van Dyk, D. A., DeGennaro, S., Stein, N., Jefferys, W. H., & von Hippel, T. 2009, *Annals of Applied Statistics*, 3, 117
- von Hippel, T., Jefferys, W. H., Scott, J., Stein, N., Winget, D. E., DeGennaro, S., Dam, A., & Jeffery, E. 2006, *ApJ*, 645, 1436
- von Hippel, T., & Sarajedini, A. 1998, *AJ*, 116, 1789
- von Hippel, T., Steinhauer, A., Sarajedini, A., Deliyannis, C. P. 2002, *AJ*, 124, 1555
- Yi, S., Demarque, P., Kim, Y.-C., Lee, Y.-W., Ree, C. H., Lejeune, Th., & Barnes, S. 2001, *ApJS*, 136, 417

Table 1.

filters	prescription	$\Delta(\text{age})$ Gyr	$\Delta([\text{Fe}/\text{H}])$ dex	$\Delta(\text{m-M})$ mag	$\Delta(A_V)$ mag
UB	Bessell 2	−0.04 (0.13)	0.01 (0.012)	−0.03 (0.014)	0.06 (0.041)
UB	Maiz-Apellaniz	−0.38 (0.14)	−0.03 (0.011)	−0.02 (0.019)	0.33 (0.040)
UBV	Bessell 2	1.03 (0.12)	0.03 (0.006)	−0.07 (0.012)	−0.13 (0.013)
UBV	Maiz-Apellaniz	1.64 (0.06)	0.05 (0.005)	−0.09 (0.011)	−0.14 (0.009)
UBVRI	Bessell 2	0.11 (0.06)	0.01 (0.004)	−0.02 (0.008)	−0.03 (0.005)
UBVRI	Maiz-Apellaniz	0.42 (0.05)	0.05 (0.003)	−0.05 (0.007)	−0.04 (0.005)

Note. — All values are relative to the first Bessell prescription.